

FUNNEL FLOW OF A NAVIER-STOKES-FLUID WITH POTENTIAL APPLICATIONS TO MICROPOLAR MEDIA

Mariia Fomicheva^{1,2}, Wolfgang H. Müller³, Elena N. Vilchevskaya^{1,2},
Nikolay Bessonov^{1,2}

¹Institute for Problems in Mechanical Engineering of the Russian Academy of Sciences,
St.-Petersburg Russia

²Peter the Great Saint-Petersburg Polytechnic University, St.-Petersburg Russia

³Institut für Mechanik, Kontinuumsmechanik und Materialtheorie, Technische
Universität Berlin, Germany

Abstract. *In this paper foundations are laid for a future solution of a fully coupled flow problem for the micropolar medium undergoing structural change in a funnel-shaped crusher. Initially the fundamental equations of micropolar media are revisited and the problem of structural changes of micropolar media moving in a crusher is explained. Then a review of the current state-of-the-art is presented and a necessary extension of the problem is motivated. The need for using numerical methods of fluid mechanics is emphasized. As a prerequisite for the study of the fully coupled initial boundary value 2D-flow problem of a micropolar fluid the funnel flow of a Navier-Stokes fluid is investigated based on an implicit finite difference scheme using the Thomas algorithm. Numerical results for velocities, stresses, and for the pressure dependence of the funnel flow are presented. The correctness of the algorithm is checked by specializing to the case of a flow through a tunnel of constant cross-section under the influence of gravity, for which an analytical solution is available.*

Key Words: *Micropolar media, Structural change, Microinertia, Viscous medium*

Received April 01, 2019 / Accepted June 14, 2019

Corresponding author: Wolfgang H. Müller

Institut für Mechanik, Kontinuumsmechanik und Materialtheorie, Technische Universität Berlin,

Sekr. MS. 2, Einsteinufer 5, 10587 Berlin, Germany

E-mail: wolfgang.h.mueller@tu-berlin.de

1. MICROPOLAR MEDIA UNDERGOING STRUCTURAL CHANGE

1.1. Introductory remarks

Generalized Continuum Theories (GCTs) have gained the attention of the materials science community because they allow modeling of materials with an inner structure. These are used in modern engineering constructions on the large as well as on the small scale, for example, in light-weight aerospace, automotive, microelectronic, and micromechanical designs. A particular type of GCT describes micropolar media, and emphasizes the aspect of inner rotational degrees of freedom of a material (see [1] for a modern formulation). This theory is particularly suited for studies of soils, polycrystalline and composite matter, granular and powder-like materials, porous media and foams and, in particular, for materials that are “somewhere in-between a solid or a fluid,” for example liquid crystals.

The following should be noted. It is well known that the inertia tensor of a continuum particle, \mathbf{J} , the so-called micro-inertia tensor, plays an important role in context with its rotational degree of freedom, specifically in combination with the angular velocity vector, $\boldsymbol{\omega}$, assigned to the continuum element. In Eringen’s theory of micropolar media (see for example [2]) \mathbf{J} is a conserved field quantity, unable of structural change and production, and not truly an independent variable such as the mass density, which characterizes the inertia of matter w.r.t. linear momentum and obeys its own kinetic equation (the mass balance), independently of the momentum balance. Therefore, most recently, it has been emphasized in [3] that the inertia tensor should also be treated as a completely independent structural field variable. However, in contrast to the balance of mass, the micro-inertia tensor is not conserved. Rather its governing equation contains a production term, $\boldsymbol{\chi}$, which within the framework of continuum theory must be considered as a constitutive quantity. In the following subsections it will be shown that it allows modeling additional features of materials, namely processes accompanied by a considerable structural change. The problem of a funnel flow will be used for demonstration, which can eventually will be investigated and later used for crushing of particles to smaller size. Previously similar problems were considered in the articles [4-7].

1.2. Governing equations

The motion of micropolar media is described by the following coupled system of differential equations:

- balance of mass,

$$\frac{\delta \rho}{\delta t} + \rho \nabla \cdot \mathbf{v} = 0, \quad (1)$$

- balance of momentum,

$$\rho \frac{\delta \mathbf{v}}{\delta t} = \nabla \cdot \boldsymbol{\sigma} + \rho \mathbf{f}, \quad (2)$$

- balance of spin,

$$\rho \mathbf{J} \cdot \frac{\delta \boldsymbol{\omega}}{\delta t} = -\boldsymbol{\omega} \times \mathbf{J} \cdot \boldsymbol{\omega} + \nabla \cdot \boldsymbol{\mu} + \boldsymbol{\sigma}_x + \rho \mathbf{m}, \quad (3)$$

where ρ is the field of mass density, \mathbf{v} and $\boldsymbol{\omega}$ are the linear and angular velocity fields, $\boldsymbol{\sigma}$ is the nonsymmetric Cauchy stress tensor, \mathbf{f} is the specific body force, \mathbf{J} is the specific

micro-inertia tensor, $\boldsymbol{\mu}$ is the non-symmetric couple stress tensor, $(\mathbf{a} \otimes \mathbf{b})_{\times} = \mathbf{a} \times \mathbf{b}$ is the Gibbsian cross, and \mathbf{m} are specific volume couples. We denote by

$$\frac{\delta(\cdot)}{\delta t} = \frac{d(\cdot)}{dt} + (\mathbf{v} - \mathbf{w}) \cdot \nabla(\cdot) \quad (4)$$

the substantial derivative of a field quantity, $d(\cdot)/dt$ is the total derivative and \mathbf{w} the mapping velocity of the observational point (see [8]).

In the traditional micropolar theory, each material point or “particle” of a micropolar continuum is phenomenologically equivalent to a rigid body. Hence, its micro-inertia does not change intrinsically, see for example [2, 9-11]. Even if a so-called micromorphic structure is considered, which in principle allows an intrinsic change of micro-inertia (following [2, 12, 13]), many papers use only the following additional equation for the conservation of inertia (*e.g.*, see [14, 15]), which is an identity:

$$\frac{\delta \mathbf{J}}{\delta t} = \boldsymbol{\omega} \times \mathbf{J} - \mathbf{J} \times \boldsymbol{\omega} . \quad (5)$$

Note that the terms on the right hand side characterize the change of the inertia tensor, which is exclusively due to rigid body rotation.

An extension to this approach was suggested in [16], where it was assumed that the inertia of polar particles may change as the continuum deforms. This idea was further elaborated in [3], where it was clearly stated that the tensor of inertia should be treated as an independent field. Within that approach a fixed elementary volume V was treated as a micropolar (macro-) particle, as customarily done in spatial description. Then its tensor of inertia is obtained by homogenization, namely by averaging the inertia tensors of micro-particles within a representative volume. Because of the movement of the medium, the elementary volume contains different micro-particles as time passes, and the inertia tensor of the volume will change due to the incoming or outgoing flux of inertia. However, internal structural transformations are also possible. These are due to combination or fragmentation of particles during mechanical crushing, to chemical reactions, or to changes of anisotropy of the material. These effects are explained in greater detail in [7, 17, 18]. In a nutshell, on the continuum scale all of this can be taken into account by adding a source term, $\boldsymbol{\chi}$, to the right-hand side of Eq. (5), which now reads:

$$\frac{\delta \mathbf{J}}{\delta t} = \boldsymbol{\omega} \times \mathbf{J} - \mathbf{J} \times \boldsymbol{\omega} + \boldsymbol{\chi} . \quad (6)$$

On the continuum level this source term must be considered as a new constitutive quantity for which an additional constitutive equation has to be formulated. The form of the constitutive equation depends on the problem under consideration and can be a function of many physical quantities, such as temperature, pressure, flow rate, etc. We will now discuss an example pertinent to the intentions of this paper.

1.3. The crusher problem: An example for structural change in a micropolar medium

A first non-trivial solution to the so-called crusher problem was presented in [7], where the situation depicted in Fig. 1 (left inset) was analyzed: Within an infinite one-dimensional space, $-\infty < x < +\infty$, a continuous flow of randomly oriented and randomly

sized micro-particles is coming in from the left. On a continuum level this corresponds to a spherical tensor of microinertia of a fixed initial size. They keep moving to the right at a constant speed, v_0 , prescribed by a conveyor belt. In other words, the balance of linear momentum does not need to be considered. It is identically satisfied. On its way to the right the particles enter a region $-\delta \leq 0 \leq +\delta$, symmetrically arranged around the position $x = 0$, where they are continuously crushed to smaller and smaller sizes. On the continuum scale this means that the tensor of micro-inertia stays spherical but that its “size” decreases.

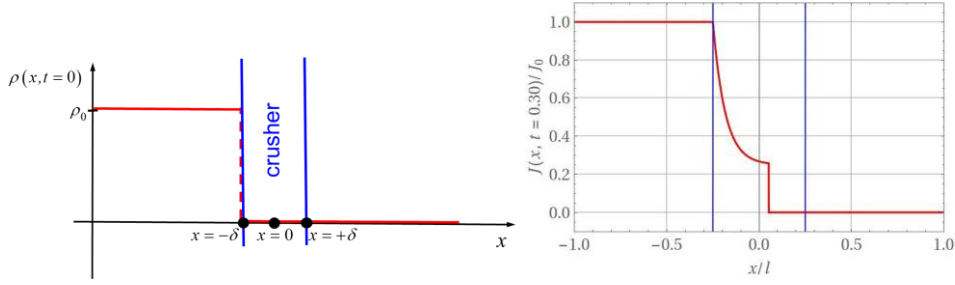


Fig. 1 1D crusher problem and microinertia development

For the production of the moment of inertia, $\chi = \chi \mathbf{I}$ the following relationship was postulated [7]:

$$\chi(x, t) = \begin{cases} 0 & \text{if } x \in (-\infty < x < -\delta) \\ -\alpha[J(x, t) - J_*] & \text{if } -\delta \leq x \leq x_f \\ 0 & \text{if } x_f < x \leq +\delta \\ 0 & \text{if } +\delta < x < +\infty \end{cases}, \quad (7)$$

where J_* and α are positive constants, which can intuitively be interpreted as being related to the minimum grain size the particles can be crushed to and to the inverse of the particle toughness, respectively. Thus, because they are characteristics of the material and not of the crusher, they are constitutive properties. x_f is the current location of the incoming shock front of the to-be-crushed particles. Note that the front will eventually leave the crusher area. For this case Eq. (6) can be solved in closed form using the method of characteristics. A typical result of the decreasing micro-inertia is shown in Fig. 1, right. It should be emphasized that the predicted change in micro-inertia is an important result in itself. It is not necessarily connected to a concurrent solution for the angular velocity ω based on the balance of spin shown in Eq. (3). In fact in the present and in the cited articles of the authors the spin balance was not touched at all. The presence of the linear velocity is sufficient to induce further change of \mathbf{J} as we shall see now.

In [5] the crusher model was extended in two ways: A transient *two-dimensional* flow of the Couette type of a *viscous* medium of the Navier-Stokes type between two plates was considered, Fig. 2.

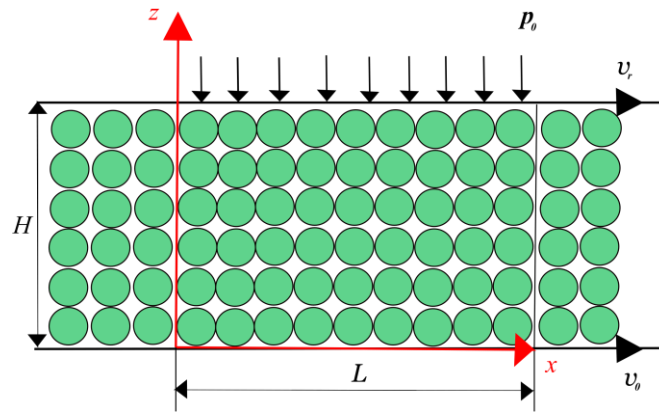


Fig. 2 Crushing of a viscous material

In this case the production term is also isotropic. It was assumed that it is given by the following expression:

$$\chi = -\alpha \text{Tr} \sigma (J - J_*) (H(x) - H(x - L)) \mathbf{I}, \tag{8}$$

where $H(x)$ is the Heaviside step function. Moreover, the “pressure” term, $\text{Tr} \sigma$, describes the conversion of the crusher action to a material response. In other words, it is related to the effectiveness of the crusher and to the transmission of its external forces into the material to be crushed.

It is important to note that the problem decouples and that it was solved (numerically) in two steps, as follows. First, the velocity is determined numerically from the transient balance of momentum Eq. (2) by using the Navier-Stokes law without bulk viscosity,

$$\sigma = -p \mathbf{I} + \eta \text{dev}(\nabla \otimes \mathbf{v} + \mathbf{v} \otimes \nabla), \tag{9}$$

where η is the shear viscosity coefficient, and p is the pressure. Then, once the velocity profile is known, it can be used to determine the temporal development of the micro-inertia by a numerical solution of Eq. (6). Typical results in dimensionless form, $\bar{v} = v/v_0$, $\bar{z} = z/H$, $\bar{t} = v_0 t/L$, $\bar{J} = J/J_0$, are shown in Fig. 3.

A few comments are made in order to explain why a viscous constitutive equation is used in context with particle crushing. There are several reasons. First, crushing of (brittle) particles is often achieved in a slurry, which is viscous due to the added water. However, even if there is no water added, the particles will be in contact with each other giving rise to friction on the mesoscopic and to viscosity on the macroscopic scale. In fact, this is also acknowledged in the literature on crushing (see [4]).

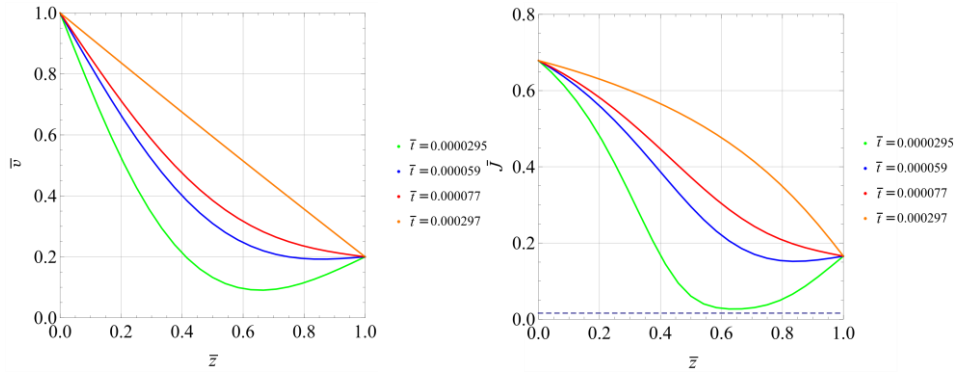


Fig. 3 Temporal development of the velocity and of the micro-inertia (horizontally at $\bar{x} = 2/3$) profiles

Consequentially, the next complication added to our crusher analysis should be the solution of a fully coupled problem, where the balances of momentum and of micro-inertia are solved concurrently. This type of problem arises, for example, during funnel flow of a viscous medium subjected to gravity (see Fig. 4). It can only be solved numerically, unless the funnel angle degenerates to $\alpha = 90^\circ$. In this paper the fully coupled problem will not be treated. In the first step we will only concentrate on the numerical solution for the flow of a viscous medium of the Navier-Stokes type without micro-inertia through a funnel. The situation will be explained in more detail in the next section.

2. PROBLEM STATEMENT

Consider the (planar) situation shown in Fig. 4. A continuous stream of bulk material flows from the top into the inlet orifice of a container of width $2L$ of height H_1 . The size of the particles entering the container region will be the same. It will also stay the same during the passage, because in this paper we consider the flow problem only and not its coupling to microinertia. Therefore, as a boundary condition we assume that the infinite supply of particles enters the system with the same velocity pointing only in y -direction,

$$\mathbf{v}(x, y = H_1 + H_2) = -v_0 \mathbf{e}_y, \quad (10)$$

at all times. We assume that the material is pushed into the tunnel under a pressure p_0 . Then the material finally enters a funnel region of height H_2 where the width narrows down linearly to $2L_0$. In this configuration the angle between the walls of the funnel and of the horizon is given by $\alpha = \arctan 1 = 45^\circ$. Gravity points in negative vertical direction,

$$\mathbf{f} = -g \mathbf{e}_y. \quad (11)$$

It attempts to accelerate the flow but, as we shall see, because of the viscous nature of the fluid the released potential energy will dissipate and the fluid is not accelerated as much as it could if there were no dissipation. As we shall explain later, it reaches a stationary state in the case of a long straight tunnel without a funnel, independently of falling

coordinate y . Note that because of the planar nature of the presented problem there will never be a velocity component out-of-plane.

Hence initially the vertical component is constant, $v_y = v_0$, and the projection of the velocity on the x -axis vanishes, $v_x = 0$. This will definitely change when the material enters the funnel region of height H_2 . Here we will encounter both velocity components,

$$\mathbf{v} = v_x(x, y, t)\mathbf{e}_x + v_y(x, y, t)\mathbf{e}_y. \tag{12}$$

We will now discuss the equations required to determine both velocity components.

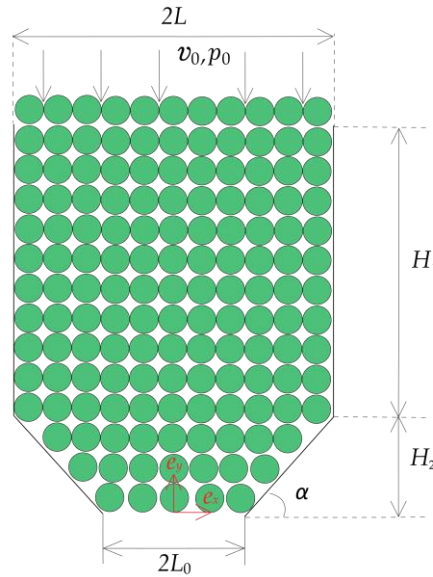


Fig. 4 Particle transport through the 2D-container

The flow we consider is that of a viscous material of the Navier-Stokes type without bulk viscosity according to Eq. (9). As it was mentioned above, the velocity cannot be regarded as constant and must be determined from the balance of linear momentum Eq. (2). It is also assumed that the liquid under consideration is incompressible, satisfying the equation

$$\nabla \cdot \mathbf{v} = 0. \tag{13}$$

Given Eqs. (9) and (13), Eqs. (2) take the form (ρ_0 is the constant mass density and the velocity \mathbf{w} of the observational point will be zero in the present case),

$$\rho_0 \frac{\delta \mathbf{v}}{\delta t} = -\nabla p + \eta \Delta \mathbf{v} + \rho_0 \mathbf{f}. \tag{14}$$

On the left and right borders of the channel, and in particular in the funnel region, no slip conditions are assumed,

$$v_y = 0, v_x = 0. \tag{15}$$

The following equations were used as boundary conditions for the pressures on the upper boundary of the system and at the end of the funnel, respectively ($H = H_1 + H_2$):

$$p(x, y = H, t) = p_0, \quad p(x, y = 0, t) = 0. \quad (16)$$

In general, Eqs. (13)-(16) are evaluated numerically by using the explicit method of integration (see [19] for a detailed explanation of the numerical method that was used). However, for a special case it is possible to check the numerical results by means of an analytic steady-state solution. Simply consider a straight tunnel of width $2L$. In other words, put $\alpha = 90^\circ$ in Fig. 4. Then consider stationary conditions and solve Eqs. (13)-(15) with the following semi-inverse ansatz:

$$\mathbf{v} = v_y(x, y)\mathbf{e}_y. \quad (17)$$

Because of the incompressibility it turns out that this velocity profile must be independent of height, meaning of the coordinate y (far from the top inlet) and is given by:

$$v_y = -(q + \rho_0 g) \frac{1}{2\eta} (L^2 - x^2), \quad (18)$$

where

$$\frac{\partial p}{\partial y} = \text{const.} = q, \quad (19)$$

and $2L$ denotes the width of the tunnel. This solution shows that the medium is not accelerated such that the velocity in y -direction increases steadily. Rather it reaches a stationary state because the released potential energy is dissipated. From a force-related viewpoint one might say that the gravitational forces acting on the bulk, the pressures acting on top and on the bottom, and the frictional forces are in static equilibrium.

3. RESULTS

We first present the transition to the stationary state based on a numerical solution of Eqs. (13)-(15). For this purpose the following (quasi-dimensionless) data was used (Δ indicates grid and time spacings):

$$\begin{aligned} L = 1, \quad H = 4, \quad q = 0.25, \quad v_0 = 0.01, \quad \rho_0 = 1.32, \quad g = 1, \quad \eta = 0.01, \quad H_1 = 3.36, \\ H_2 = 0.64, \quad L_0 = 0.36, \quad \Delta x = 0.04, \quad \Delta y = 0.04, \quad \Delta t = 1. \end{aligned} \quad (20)$$

Fig. 5 shows a comparison of stationary situations for a direct channel for a cross-section $y = 1/2H$. It can be seen that the analytical solution (18) and the numerical solution are in good agreement with each other.

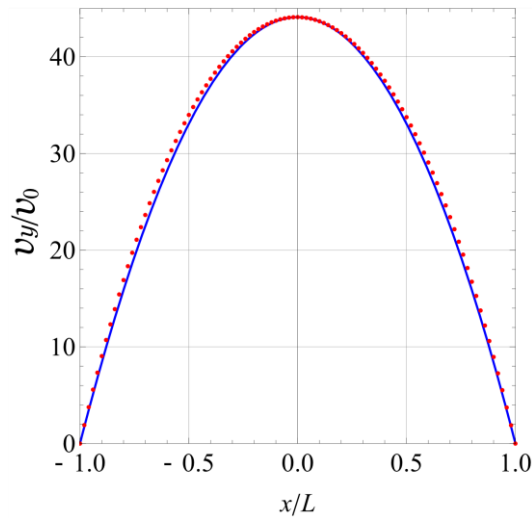


Fig. 5 Distribution of the vertical velocities. Comparison of analytical and numerical solutions (solid and dotted lines, respectively)

The following figures show the distribution of the velocity projections on the x - and y -axes in various cross-sections at different points of time. Note that the graphs are presented in dimensionless form. Velocities shared initial velocity v_0 on the upper border of the vessel (since the initial velocity was directed against the y -axis, then v_0 is a negative value). The axis y was divided by H_2 , and the axis x by L . Also note that all calculations were performed for $\alpha = 45^\circ$.

The three insets on the left of Fig. 6 show the distribution of the horizontal velocity component v_x as a function of height h as time passes, $t_1 < t_2 < t_3$. The following can be said about the horizontal velocity components $v_x(x, y, t)$:

- They are antisymmetric w.r.t. $x = 0$: $v_x(x, y, t) = -v_x(-x, y, t)$. This is why only half of the distribution is shown.
- They vanish at the wall as they should.
- They become smaller with increasing height y , which makes sense because they result as a consequence of a narrowing cross-section.
- They increase with time and a stationary state (if it exists) has not been reached at time t_3 yet.

The insets on the right of Fig. 6 show the distribution of vertical velocity component v_y as a function of height h . The following can be said about the vertical velocity components $v_y(x, y, t)$:

- They are mirror-symmetric w.r.t. $x = 0$: $v_y(x, y, t) = v_y(-x, y, t)$.
- They vanish at the wall and at $x = 0$ as they should.
- They become smaller with increasing height y , which we expect because there is more space for the fluid. Also with increasing height y they look parabolic, which makes sense for a Hagen-Poiseuille type of flow.
- They increase with time and a stationary state (if it exists) has not been reached at time t_3 yet.

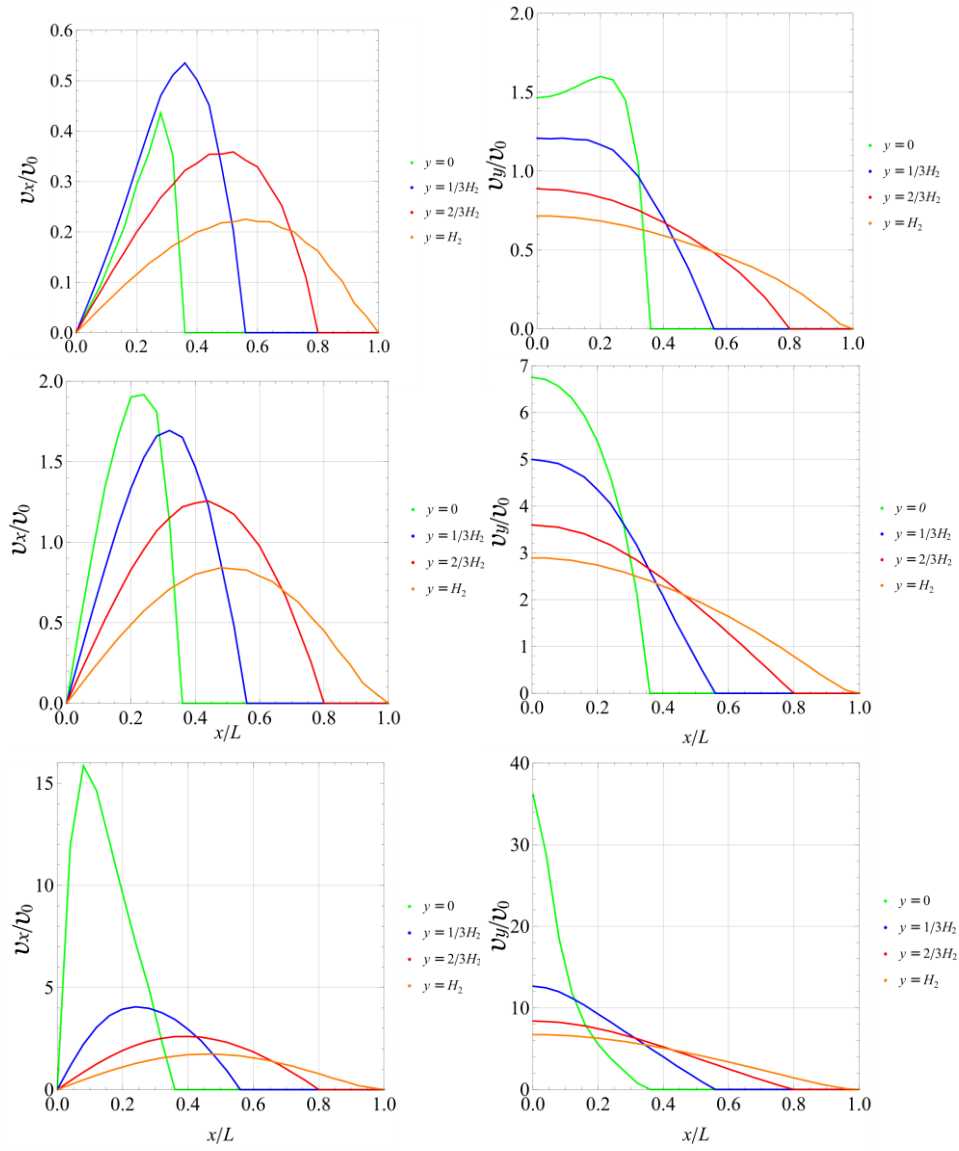


Fig. 6 Distribution of the horizontal and of the vertical velocities (left and right insets, respectively) at increasing times at various vertical cross-sectional heights y

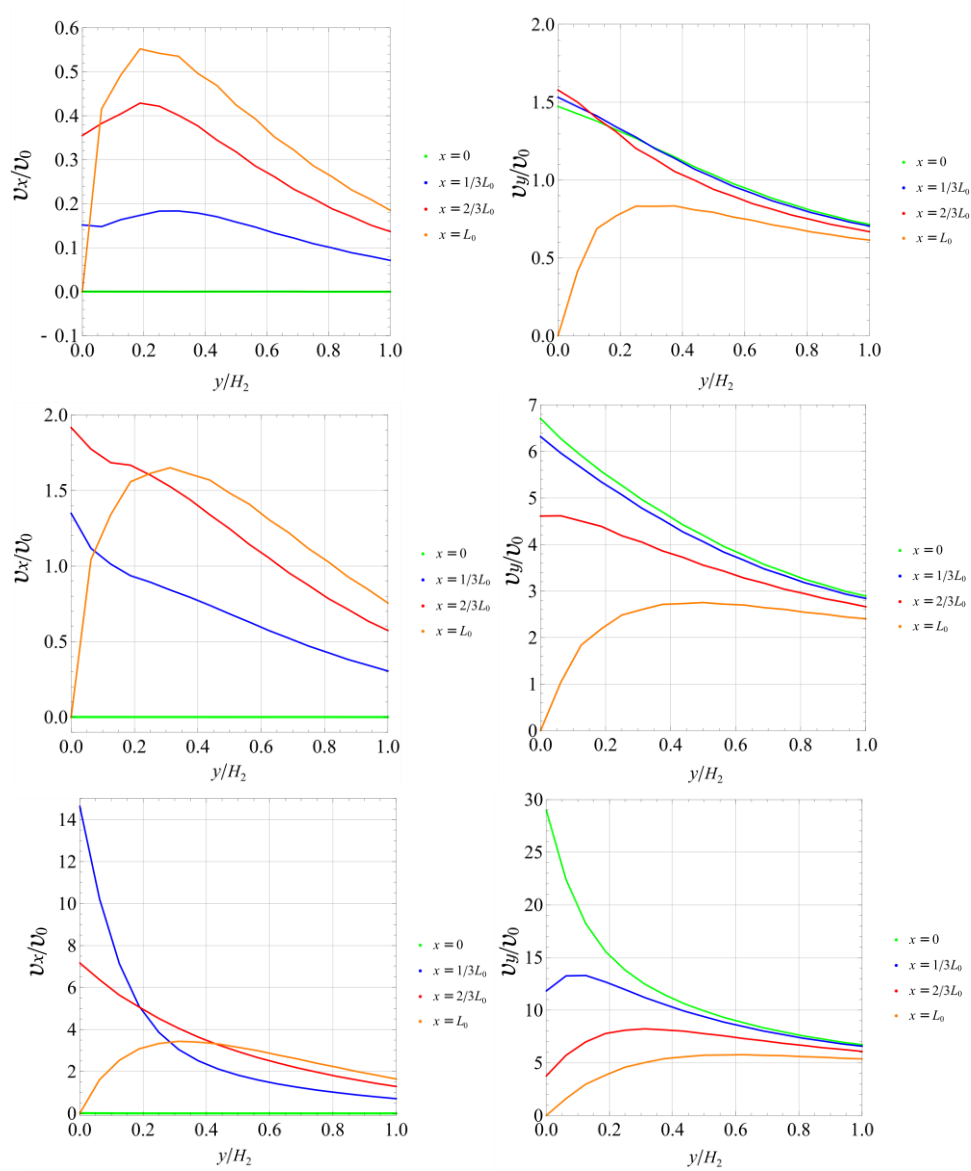


Fig. 7 Distribution of the horizontal and of the vertical velocities (left and right insets, respectively) at increasing times at various horizontal cross-sectional cuts x

Fig. 7 presents essentially the same information as the two previous sets of figures but from a different viewpoint. Now both velocity components are depicted as a function of “falling height” y for various cross-sectional cuts. For the horizontal component $v_x(x, y, t)$ the following can be said in addition to the previous statements:

- For greater heights y the velocities increase if one moves away from the center towards $x = L$.
- At smaller heights the behavior is more complex. In particular the curve at position $x = L$ describing the situation at the end of the funnel, ($y = 0$) must go through zero, because of the boundary condition.
- Some curves are slightly jaggedly, which is because the points of integration were connected by linear lines, which does not depict the situation correctly.

For the horizontal component $v_x(x, y, t)$ the following can be said in addition to the previous statements:

- The velocities in the middle $x = L$ are the greatest, as to be expected.

Fig. 8 shows the distribution of pressure isolines in the vessel at different points in time. In contrast to Fig. 4 the container was rotated by 90 degrees for convenience of graphical representation. The direction of flow is indicated by an arrow. Note that the greater the pressure, the brighter the isolines. These distributions will become important as a measure of the intensity of the crushing process in view of the equation for the production of microinertia shown in Eq. (8). Obviously there is now high potential for crushing or better microinertia production in the narrowing funnel. In contrast to that nothing will happen in the straight passageway.

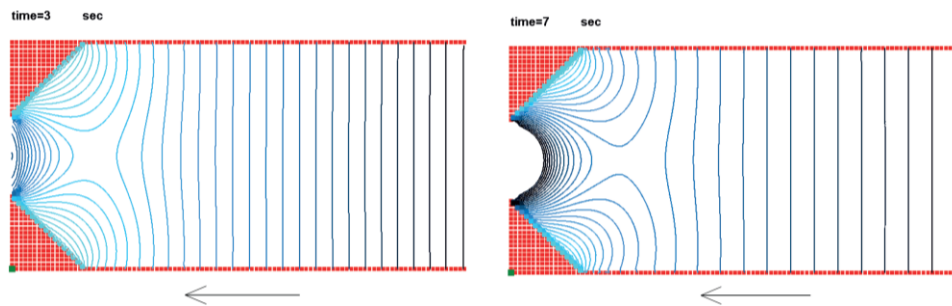


Fig. 8 The distribution of the pressure isolines in the vessel at different points of time

4. CONCLUSIONS AND OUTLOOK

In this paper the following was achieved:

- The importance of studying micropolar media as an example of a generalized theory of continuum was emphasized, since they allow modeling materials with an internal structure besides taking into account the aspect of the internal rotational degrees of freedom of the material. This theory is suitable for studying many applied problems, for example, in soil mechanics.
- An extension of the balance of microinertia was presented. It accounts for due intrinsic structural changes of microinertia and the need for the extension was physically motivated.
- As a particular example of this kind of problem, the milling process in a crusher was used.

- As a prerequisite for further study the flow of a Navier-Stokes fluid through a 2D-funnel was investigated numerically.
- Velocities and pressure distributions were obtained, discussed, and may now serve for future studies of the coupled problem of the funnel flow of a micropolar medium showing structural change due to milling.

Acknowledgements: Support of this work through a stipend from TU Berlin to M.F. is gratefully acknowledged.

REFERENCES

1. Eremeyev, V.A., Lebedev, L.P., Altenbach, H., 2012, *Foundations of micropolar mechanics*, Springer Science & Business Media, Heidelberg, New York, Dordrecht, London.
2. Eringen, A.C., Kafadar, C.B., 1976, *Polar field theories*, In: *Continuum physics IV*, Academic Press, London.
3. Ivanova, E.A., Vilchevskaya, E.N., 2016, *Micropolar continuum in spatial description*, *Continuum Mechanics and Thermodynamics*, 28(6), pp. 1759-1780.
4. Bain, O., Billingham, J., Houston, P., Lowndes, I., 2015, *Flows of granular material in two-dimensional channels*, *Journal of Engineering Mathematics*, 98(1), pp. 49-70.
5. Fomicheva, M., Vilchevskaya, E.N., Müller, W., Bessonov, N., 2019, *Milling matter in a crusher: Modeling based on extended micropolar theory*, *Continuum Mechanics and Thermodynamics* (in print).
6. Glane, S., Rickert, W., Müller, W.H., Vilchevskaya, E., 2017, *Micropolar media with structural transformations: Numerical treatment of a particle crusher*, *Proceedings of XLV International Summer School — Conference APM 2017*, pp. 197-211.
7. Müller, W.H., Vilchevskaya, E.N., Weiss, W., 2017, *A meso-mechanics approach to micropolar theory: A farewell to material description*, *Physical Mesomechanics*, 20(3), pp. 13-24.
8. Ivanova, E., Vilchevskaya, E., Müller, W.H., 2016, *Time derivatives in material and spatial description – What are the differences and why do they concern us?*, in K. Naumenko, M. ABmus (Eds.), *Advanced Methods of Mechanics for Materials and Structures*, pp. 3-28, Springer.
9. Eringen, A., 1997, *A unified continuum theory of electrodynamics of liquid crystals*, *International Journal of Engineering Science*, 35(12-13), pp. 1137–1157.
10. Truesdell, C., Toupin, R.A., 1960, *The classical field theories*, Springer, Heidelberg.
11. Mindlin, R., 1964, *Micro-structure in linear elasticity*, *Archive of Rational Mechanics and Analysis*, 16(1), pp. 51-78.
12. Eringen, A., 1976, *Continuum Physics*, Vol. IV, Academic Press, New York.
13. Eringen, A., 1999, *Microcontinuum Field Theory I*, *Foundations and Solids*, Springer, New York.
14. Oevel, W., Schröter, J., 1981, *Balance equation for micromorphic materials*, *Journal of Statistical Physics*, 25(4), pp. 645–662.
15. Chen, K., 2007, *Microcontinuum balance equations revisited: The mesoscopic approach*, *Journal of Non-Equilibrium Thermodynamics*, 32(4), pp. 435-458.
16. Dłuzewski, P.H., 1993, *Finite deformations of polar elastic media*, *International journal of solids and structures*, 30(16), pp. 2277-2285.
17. Müller, W.H., Vilchevskaya, E.N., 2018, *Micropolar theory with production of rotational inertia: A rational mechanics approach*, *Generalized Models and Non-classical Approaches in Complex Materials*, 1, pp. 195-229. Springer, Cham.
18. Morozova, A.S., Vilchevskaya, E.N., Müller, W.H., Bessonov, N.M., 2019, *Interrelation of heat propagation and angular velocity in micropolar media*, *Dynamical Processes in Generalized Continua and Structures*, pp. 413-425. Springer, Cham.
19. Chorin, A.J., 1997, *A numerical method for solving incompressible viscous flow problems*, *Journal of computational physics*, 135(2), pp. 118-125.